Modelling approaches of the in-plane shear behaviour of unreinforced and FRP strengthened masonry panels

A. Gabor [a], A. Bennani [a], E. Jacquelin [a,*], F. Lebon [b]

[a] *Laboratoire Mécanique Matériaux, Université Claude Bernard Lyon1, 82, Boulevard Niels Bohr, Campus de la DOUA, 69622 Villeurbanne Cedex, France*

[b] *Laboratoire de Mécanique et d'Acoustique, CNRS, 31, Chemin Joseph-Aiguier, 13402 Marseille Cedex 20, France*

The paper presents different finite element modelling approaches, developed with a commercial software, for the analysis of the behaviour of unreinforced and FRP strengthened masonry walls when their are subjected to a predominant shear load. Three models are analyzed, having different complexity levels. These models are used for the simulation of diagonal compression tests on masonry panels. The numerical simulations are compared with experimental results and the reliability of the different finite element models is discussed.

Keywords: Hollow brick masonry; FRP reinforcement; Non-linear shear behaviour; Finite element modelling; Homogenization

1. Introduction

Large populations of masonry buildings situated in seismic zones have not been designed and built for seismic loading; therefore the assessment of the vulnerability of these structures and their seismic upgrade is a current problem with important socio-economic implications. In order to answer this challenge, retrofitting techniques and assessment methods are continuously improved.

Nowadays, research focuses on innovative strengthening techniques, involving fiber reinforced polymer (FRP) materials. FRPs are made of strong fibers of carbon or glass bonded together with a polymeric matrix. These materials offer a high strength and stiffness in the direction of the fibers and increased strength-to-weight ratio. A state-of-the-art of the FRP strengthening of civil engineering structures is presented in [1–3]. The main objective of the reinforcement is to enhance the earthquake resistance of masonry structural elements, in order to avoid failure modes that manifest in brittle and unforeseen manner. The behaviour and damage pathology of masonry walls submitted to predominant shear load is classified in this category [4]. Generally, the behaviour of masonry structures or masonry structural elements is approached considering the out-of-plane or the in-plane behaviour.

Experimental studies concerning the out-of-plane flexural strength and deformation capability were conducted by Ehsani et al. on half scale brick walls strengthened with FRP composite strips [5]. In a similar study [6], the influence of several experimental parameters on the load carrying capacity of carbon-FRP reinforced panels are investigated: the type, amount, layout of the reinforcement and the effects of a moderate compressive axial load.

Concerning the in-plane behaviour, Corradi et al. [7] pursued a comparative in situ study of the effectiveness of different strengthening procedures applied to ancient stone masonries. In the same context, Valluzzi et al. [8]

* Corresponding author. Tel.: +33 4 72 69 21 30; fax: +33 4 78 94 69 06.

E-mail address: jac@iutal2m.univ-lyon1.fr (E. Jacquelin).

performed an experimental study in order to investigate the efficiency of an FRP shear reinforcement technique. Several reinforcement configurations were evaluated on small masonry panels submitted to diagonal compression tests.

On the basis of these studies, it appears that the use of FRP composites to retrofit unreinforced masonry walls might be an efficient alternative to enhance the wall's global out-of-plane and in-plane behaviour. However, some problems need further analysis, especially the choice of an optimized reinforcement in terms of strength, elastic moduli and layout. Additionally, the local acting mechanisms of the reinforcement strips or sheets need to be analyzed.

The finite element modelling is a currently used tool in the evaluation of the load bearing and deformation capabilities of masonry structures. Generally, two different approaches are adopted to model the behaviour of masonry elements or structures: micro- and macro-modelling.

The micro-modelling considers the masonry as a composite material built of brick units and mortar joints. Consequently, there is a large number of parameters that occur in the construction of a mechanical model: the properties of bricks and mortar, the geometry of the bricks, the joint arrangement, the interface phenomena, etc. Recent works in this field are principally devoted to the development of some reliable interface models [9] or incorporating fracture mechanics and plasticity concepts [10]. Nevertheless, the use of micro-models for the evaluation of the global behaviour of an entire masonry building is prohibitive because of the increased number of elements generated.

The macro-modelling considers the masonry as a homogeneous continuum, which replaces the brick/mortar assembly. From this point of view, we can mention the homogenized models that either take into account the tensile cracking of the masonry [11] or use constitutive equations built on anisotropic elasto-plasticity [12].

However, the prediction of the behaviour of a masonry structure or a structural element is rather delicate due to the lack of some reliable experimental data. This is usually compensated by the calibration of the numerical model, but the calibration diminishes the prediction capability of the modelling. Besides, the developed models are rarely implemented in widely distributed commercial softwares.

The aim of this paper is to analyse the reliability of a finite element modelling, developed with a commercial software in the assessment of the behaviour of unreinforced and FRP strengthened masonry walls when they are subjected to a predominant shear load. We simulate the behaviour of hollow brick masonry walls reinforced with glass and carbon fiber overlays using the ANSYS software. The modelling uses the mechanical parameters of masonry constituents determined experimentally in compression and shear. A validation is performed in the case of panels submitted to diagonal compression test. The main goal is to predict the global behaviour of the masonry walls and to evaluate the strain and damage distribution in the unreinforced and FRP strengthened panels.

In the first part of the paper we shortly present the experimental results concerning the evaluation of the mechanical parameters and to the assessment of the behaviour of the unreinforced and strengthened masonry panels which is also described. These results are used for validating the different modelling approaches presented in this paper. We recall that these results together with the employed experimental procedures are presented in more detail in previous works [13,14].

The second part of the paper is devoted to the presentation of the finite element modellings in order to analyse the behaviour of the unreinforced and the strengthened masonry panels. The models have different complexity levels:

- Detailed modelling, which considers the real configuration of the masonry panels (constituted from bricks and mortar) and the composite reinforcement. This modelling is applied in both cases (unreinforced and strengthened panels).
- Simplified modelling, considering the experimentally measured global mechanical parameters of the masonry panels.
- Simplified modelling, based on homogenization theory, where bricks and mortar are replaced by an equivalent continuum.

Finally, the finite element modelling results are compared to the experimental ones, giving place to the discussion of the reliability of the employed finite element models.

2. Mechanical properties of the constituents

The goal of the experimental evaluation of the mechanical parameters of the constituents is to obtain the values of some useful parameters that can be implemented directly in a finite element model on a commercial software, in order to simulate a specified behaviour: in our case, the behaviour of masonry panels submitted to diagonal compression loading. The diagonal compression generates a combined state of shear and compression along the direction of the horizontal and vertical joints. Thus, for the considered approach, we are interested in the evaluating of the main mechanical parameters of the masonry in compression and shear. Where it is available, the experimental procedures follow technical recommendations or standards [15, 16].

The mechanical parameters of FRP overlays were determined in uniaxial traction.

2.1. Masonry

In order to determine the elastic moduli of masonry constituents, three masonry prisms were realized and tested on the basis of the RILEM recommendation [15]. The prisms were constructed using $210 \times 100 \times 50$ mm hollow bricks and a ready-to-use mortar with a 0–5 mm sand and Portland cement composition. The water quantity added to the dry mixture was determined ensuring a good workability of the fresh mortar. The joint thickness and the brick dimensions are the same as for the masonry panels employed later for the diagonal compression test. Thus the masonry prisms can be considered as extracted from a real masonry wall.

The vertical and horizontal strains in masonry units were measured directly by strain gauges, while on the whole prism they were measured by LVDT extensometers (Fig. 1). The precision of the gauges is 1 μm/m and of the LVDT extensometers is 1 μm. The load is displacement controlled (0.5 mm/min) and measured by a 500 kN load cell.

Thus, the elastic modulus of bricks (E_b) and of a masonry prism (E_{prism}) has been determined directly using the strain measurement results, while the elastic modulus of the mortar joint (E_{mort}) was calculated using the former moduli and considering that the total vertical displacement of the prism is the sum of the displacements of the joints and of the bricks:

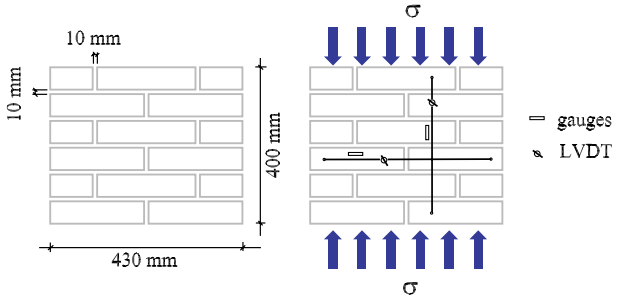

Fig. 1. Geometry and instrumentation of compression tests on prisms.

$$E_{mort} = \frac{E_{prism} E_b}{\alpha(E_b - E_{prism}) + E_b}, \quad (1)$$

where α represents the ratio of the heights of the brick and of the mortar joint.

The shear characteristics of the masonry and the brick/mortar joint interaction parameters at the interface are determined on a masonry prism (triplet). The experimental device is conceived in such a manner that it can simultaneously apply a static horizontal confinement load and a steadily increasing vertical shear load to the specimen (see Fig. 2). The loading forces are controlled by load cells; the axial load is maintained constant during the tests using a special device. Relative displacement between two adjacent bricks is measured by an LVDT device. The precision of the measurement devices is similar to the one used for the uniaxial compression test. The test results of 18 triplets for confining stresses varying from 0 to 1.8 MPa allowed us to determine the parameters of a Mohr–Coulomb constitutive equation: the shear strength and the residual friction coefficient. Quantitative results of the above mechanical parameters are presented in Table 1.

2.2. FRP reinforcement

Three types of FRP composites are employed: a unidirectional glass fiber (noted RFV), a unidirectional carbon fiber (noted RFC) and a bidirectional glass fiber (noted RFW). The mechanical properties of the composites has been determined in tension on coupons. The composite coupons are manufactured in the same conditions as they are overlayed on the walls: embedding the composite fibers in the epoxy resin. All the reinforcements reveal a linear elastic behaviour, but the

Table 1
Mechanical properties of masonry and constituents

	Bricks	Mortar	Masonry
Elastic modulus (MPa)	12,800	4000	9400
Shear strength (MPa)	–	1.63	–
Residual friction angle	–	43°	–

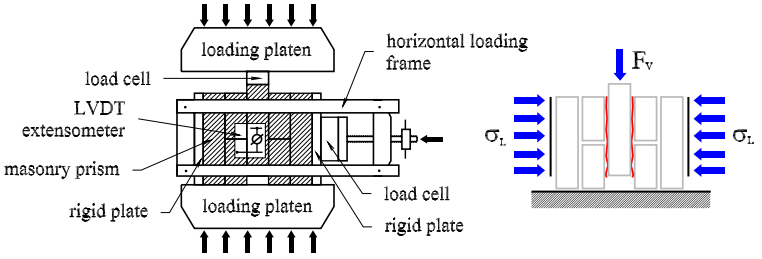

Fig. 2. Experimental setup and instrumentation of shear tests.

Table 2
Mechanical properties of the composite reinforcements

Ref.	Weighing (g/m^2)	No. of coupons	Mean thickness (mm)	Elastic modulus (MPa)		Mean strength (MPa)	Ultimate strain (%)
				E_{xx}	E_{yy}		
RFV	400	5	2.2	23,000	2500	460	2
RFC	180	5	1.9	80,000	3000	720	0.9
RFW	175	5	2.1	10,000	10,000	100	1

mechanical properties are completely different from one composite to another (see Table 2). The composites RFV and RFC can be considered as high strength and high modulus, while RFW can be considered as having low mechanical properties. Besides, the RFV composite ultimate strain is two times higher than the ultimate strain of the other composites: this property is very useful for seismic design.

3. Experimental study

3.1. Masonry panels description

The masonry panels employed for the diagonal compression tests were built according to the RILEM recommendations [16]. The size of a masonry panel is established in function of the unit size, so that the panels have a representative number of joints and units. Thus, a series of five masonry panels, having nominal dimensions of $870 \times 840 \times 100$ mm, were built (Fig. 3). They were made of hollow bricks and have a 10 mm thick mortar joint. Two of them have been kept without reinforcement, the three other panels have been strengthened with the three types of FRP composites. In order to apply the compression loading, the corners of the panels are embedded in two stiff loading shoes filled with concrete. The length of the embedding is approximately equal to the 1/6th of the wall length.

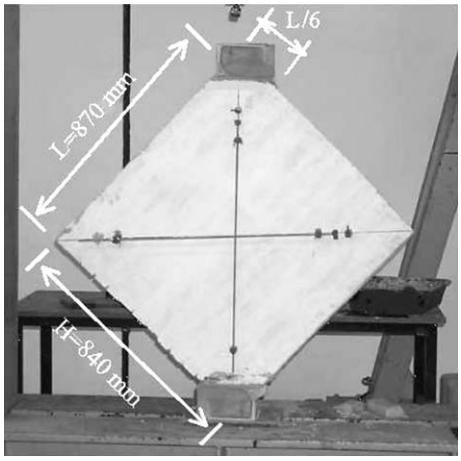

Fig. 3. Geometrical configuration and boundary conditions for masonry panels tested in diagonal compression.

In order to study the effectiveness of the different FRP composites, two configurations of the retrofit system were investigated. For the masonry panels reinforced with RFV and RFC unidirectional composites, four strips were bonded orthogonally to the loaded diagonal. The dimensions of the strips were 400×150 mm. The vertical spacing between strips is approximately 100 mm. For the third bidirectional composite (RFW), the entire surface of the panel was reinforced: the orientations of the composite fibers follow the compressed and stretched diagonals. The panels' reinforcement scheme is presented on Fig. 4. For the identification of the masonry panels, we use the same denominations as for the composites.

We remark that the choice of the reinforcement configuration is guided by the following reasons:

- Composites work efficiently only when loaded in traction; this justifies the orthogonal disposing to the compressed diagonal, the direction of the principal tensile stresses.
- The principally loaded zone is localized along the compressed diagonal, where cracks are susceptible to occur during the diagonal compression test, as confirmed later by the finite element modelling.
- The choice to keep zones unstrengthened along the compressed diagonal is guided by saving reasons.

3.2. Experimental set-up

The diagonal compression load is applied on the corners of the walls via a hydraulic actuator. The experimental setup for the diagonal compression is presented in Fig. 5. The load is gradually applied by a 500 kN hydraulic jack and controlled by a load cell. The displacements of compressed and stretched diagonals of masonry panels are measured by LVDT transducers. The experimental results are used to validate the different modelling approaches presented in the following sections, by comparing the force–strain curves of the compressed diagonals and the damage distribution in the walls. We summarize below the experimental results, which are presented and analyzed with more details in a previous work [17].

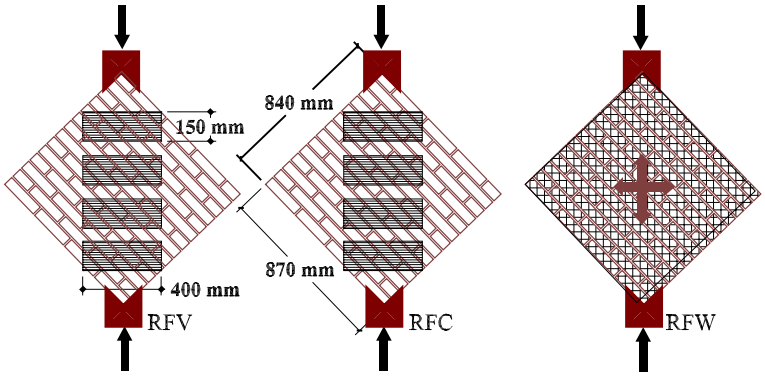

Fig. 4. Configuration of strengthening for masonry panels.

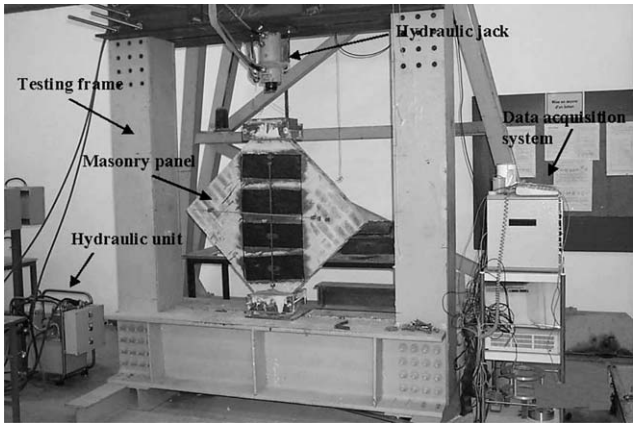

Fig. 5. Experimental setup for diagonal compression test on masonry walls.

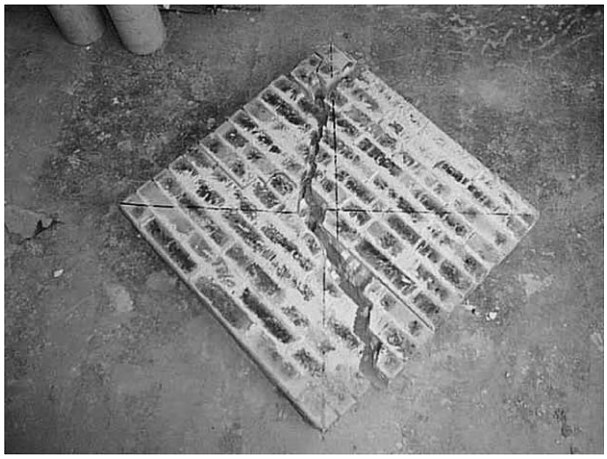

Fig. 6. Failure pattern of the masonry panel in diagonal compression.

3.3. Experimental results

The unreinforced panels present a brittle failure along the compressed diagonal, with crackings that appear suddenly in the mortar joints and in the bricks, producing the instantaneous failure of the walls (Fig. 6).

The global behaviour, described by the applied load vs. strain along the compressed diagonal curve, is quasi elastic with a very weak yield plateau (Fig. 7). The difference between the measured ultimate loads (curves NR1 and NR2) is relatively important (17%): this may be explained by the internal structure of the walls. Indeed, the failure strength is conditioned by the shear strength induced by the interaction of the mortar notches with the internal wallettes at the brick/joint interface. The random distribution and the size of the mortar notches in the hollows affect the shear strength, as it was observed on the triplet specimens during the material characterization. These tests showed dispersions of the same order.

For the strengthened masonry panels subjected to the diagonal compression, let us consider the force vs. strain curves of the tested masonry walls (Fig. 8). *NR*1, *NR*2 denote the two unreinforced masonry walls while

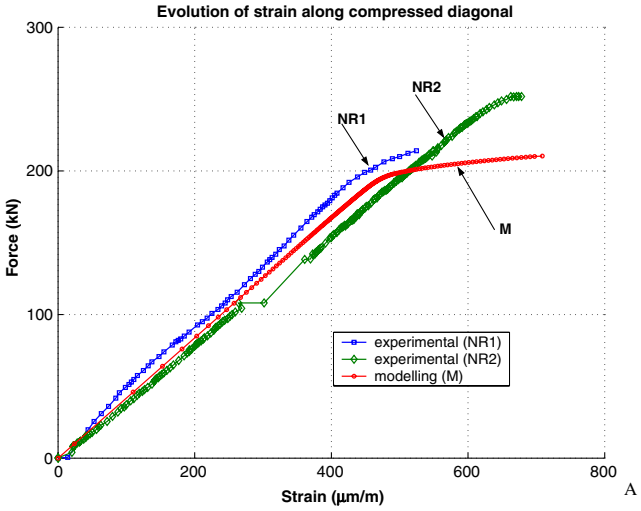

Fig. 7. Force–strain diagram of the compressed diagonal, experimental and numerical results.

RFV, RFC, and RFW denote the three reinforced walls. The elastic phases of the curves of the reinforced panels are characterized by the same slope as those obtained in

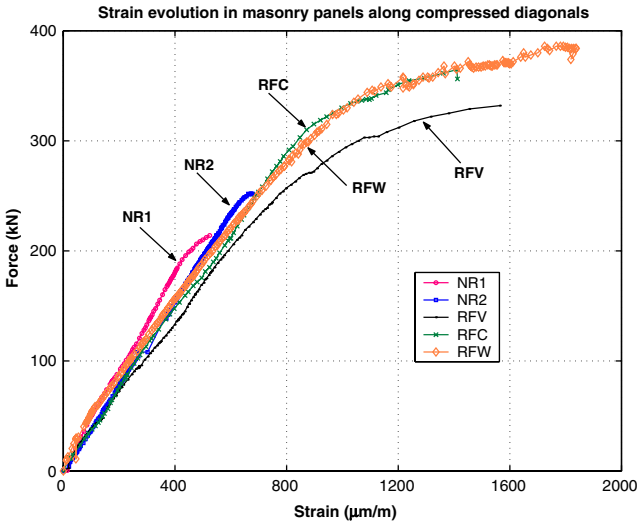

Fig. 8. Comparison of the global behaviour of unreinforced and strengthened panels: experimental results.

the case of the unreinforced ones, regardless to the type of the composite. On the other hand, the load corresponding to the elastic limit and the ultimate load of the reinforced panels are much higher than the one of the unreinforced panels. The gain in strength is quite remarkable: 42% for the RFV reinforcement and over 65% for the RFW. Thus, a first consequence of the reinforcement is the growth of the strength of the wall while its initial in-plane stiffness is kept unmodified.

Moreover, we remark an important deformation capability of the reinforced walls, emphasized by the presence of a relevant post-elastic plateau. The deformations corresponding to the maximum loads of the reinforced walls are three times higher than those of the unreinforced walls. Therefore, the seismic behaviour is enhanced. We notice also that the deformation capability of the masonry wall strengthened with the RFW composite is the best, even if the mechanical properties of the composite are the weakest. The results are summarized in Table 3.

The failure modes observed for the three walls are as follows:

Table 3
Experimental results

	Reinforcement type	Failure load (kN)	Failure mode	Ultimate strain (μm/m)
NR1	–	215.3	Diagonal splitting	470
NR2	–	251.8	Diagonal splitting	700
RFV	1D glass fiber	332.0	Splitting	1500
RFC	1D carbon fiber	361.0	Crushing	1500
RFW	2D glass fiber	384.0	Crushing	1800

- The panel reinforced with the RFV composite failed suddenly due to a cracking along the compressed diagonal at the ends of the composite strips.
- The two other walls, strengthened with RFC and RFW strips, failed locally at the compressed corners, in the loading shoes. In this latter case, the tests were stopped when some debris detached from the loading shoes.

Thus, we can conclude that the use of the composite reinforcement is quite effective under the following conditions:

- Composites having relatively weak mechanical properties but with a good deformation capability must be employed, otherwise they are not used at their full capacity.
- The geometrical arrangement of the joint/brick assemblage requires the use of bidirectional composites and the application of composite sheets onto the entire loaded zone, otherwise a brittle failure still occurs.

4. Finite element modelling of the behaviour of unreinforced masonry panels

The main goal is to evaluate the strain and damage distribution in the unreinforced and strengthened panels when their are submitted to a predominant shear load, taking into account the non-linear behaviour of the masonry. In fact, the non-linear shear behaviour of the masonry panels is mainly governed by the phenomena that occur at the brick/mortar interface (the interaction of mortar cores with the internal walettes of the bricks). However, the introduction in the model of elasto-plastic interface elements increases its complexity [9]: the construction of the model and computing time become lengthy. These considerations led us to the development of less complex models, using a commercial finite element software (ANSYS). The presentation of these models is the subject of the following paragraphs.

4.1. Detailed modelling of the unreinforced masonry

This approach considers the detailed structure of the masonry: it is built as a regular inclusion of bricks into a matrix of mortar. The mortar is considered as a net which perfectly bonds to bricks. The geometrical configuration and the boundary conditions are identical to the real ones (Fig. 9).

The bricks are fully elastic and the mortar joint is characterized by an appropriate elasto-plastic model. Thus, the non-linearity of the brick/mortar interface is transposed onto the behaviour of the mortar joint, supposing that this artifice has no effect on the global

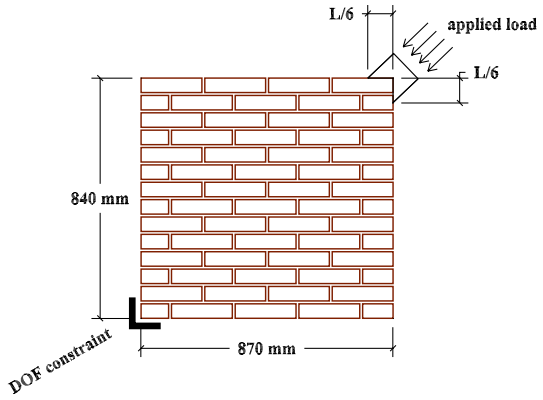

Fig. 9. Geometrical configuration of a masonry panel.

behaviour, given the low volume of mortar compared to the volume of bricks. The comparison of numerical and experimental results shows that this choice is valid. The chosen constitutive law for the modelling of the mortar joint is elastic-perfectly plastic in a Drucker–Prager formulation. This implementation lays on the Mohr–Coulomb mechanical parameters which have been experimentally determined and summarized in Table 1: the shear strength (cohesion), the residual friction coefficient and the dilatancy angle (is considered equal to zero).

A plane stress modelling is pursued using four node standard elements having two degrees of freedom per nodes, four Gauss integration points and lagrangian polynomials as shape functions. Mesh size is imposed by the relative dimensions of units and mortar: the size of the elements modelling the mortar is uniform and equal to the thickness of the joint, whereas the brick mesh size becomes coarse in their interior (Fig. 10).

This model gives a relatively good picture of the behaviour of the unreinforced masonry panel. The experimental and numerical force–strain diagrams of the compressed diagonal agree in terms of global stiffness and ultimate force (Fig. 7). The differences between experimental and numerical results are in the range of

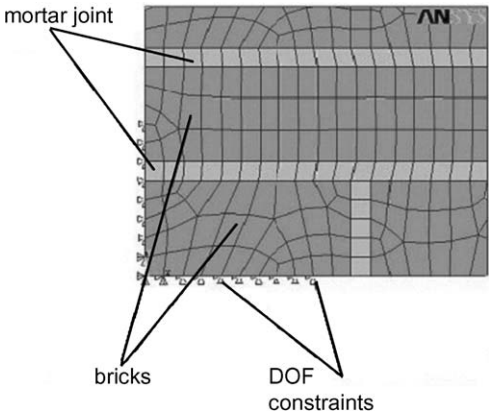

Fig. 10. Meshing detail of the masonry panel.

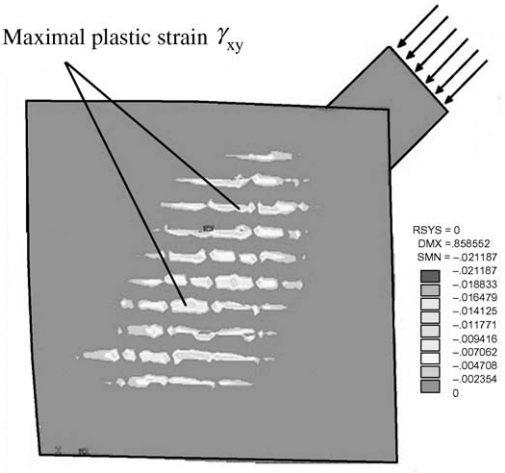

Fig. 11. Plastic shear strain distribution in the masonry (modelling result).

spreadings of experimental values obtained for the implemented mechanical parameters. When the yield is reached, we observe a sudden change of the global stiffness which predicts the degradation of the mechanical properties and the failure. The analysis of the strain distribution map reveals that the plastic strain appears and grows in the center of the panel (Fig. 11). We can consider that the failure occurs in this zone by the excess of the strain capability of the mortar joint, which agrees with the experimentally observed failure mode (Fig. 6).

4.2. Simplified modelling

The detailed modelling of the geometrical structure of the masonry requires important computational resources and renders the modelling quite laborious. Thus, if the goal of the modelling is to obtain an approximation of the average behaviour of the masonry in terms of loads and strains, it is conceivable to build an equivalent material model without considering the internal geometry of the masonry. In addition, we can consider that the influences of the different implemented parameters are independent: the elastic modulus does not act on the global resistance as well as the shear strength does not modify the global stiffness of the masonry.

In these conditions, we can propose a simplified model considering an equivalent material having the global elastic properties of the masonry panel (measured on the small masonry prisms) and the plastic parameters of the joint/brick interface (shear strength and friction coefficient). The experimental values of these parameters are summarized in Table 1.

Therefore, we considered two cases:

- Elastic-perfectly plastic isotropic wall: the considered parameters are E_{prism}, the shear strength ($\tau_{\max} = 1.63$ MPa), and the friction angle ($\phi = 43°$).

- Elastic-perfectly plastic orthotropic wall: The orthotropy of the masonry is determined by the different brick/mortar volume ratios in the directions of the bed and head joints. In a first approximation, as the mortar and brick moduli are known, this orthotropy can be expressed considering different height ratios α in the two orthogonal directions. Therefore, two elastic moduli can be calculated using the relation (1):
  (a) E^x_{prism} is used with $\alpha = 21$, so $E^x_{\text{prism}} = 11,600$ MPa;
  (b) E^y_{prism} is used with $\alpha = 5$, so $E^y_{\text{prism}} = 9400$ MPa.

For the shear modulus G^{xy}_{prism} we consider $0.3E^y_{\text{prism}}$.

The results of the simplified modellings are compared with those of the detailed geometrical modelling on the Fig. 12. We remark that the simplified isotropic and orthotropic models (referred as "isotropic" and resp. "orthotropic" on Fig. 12) give the same global stiffness, but the afferent values are lower then the value obtained by the detailed modelling (referred as "detailed" on the same figure). The difference is relatively important, about 25%. Concerning the failure loads, the values of the different elastic-perfectly plastic modellings are close, which confirms again the role of the shear strength $\tau_{\max}$ in the assessment of the ultimate load.

The isotropic elasto-plastic model is not able to localize correctly the zones with the largest strain (Fig. 13). Only the "orthotropic" elasto-plastic model gives a realistic distribution of strains along the compressed diagonal (Fig. 14). This model can be a solution for a quick detection of the zones to strengthen.

In order to improve the effectiveness of the simplified modelling in the evaluation of the global stiffness of the masonry it is necessary to perform a homogenization based on the related theory.

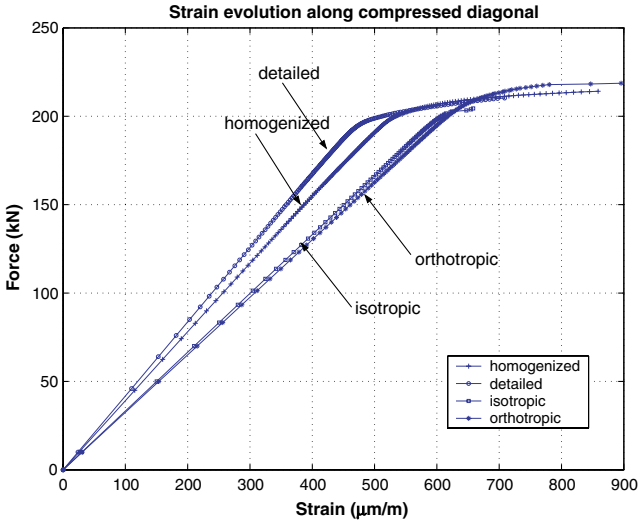

Fig. 12. Numerical results for the force–strain curves of the considered models.

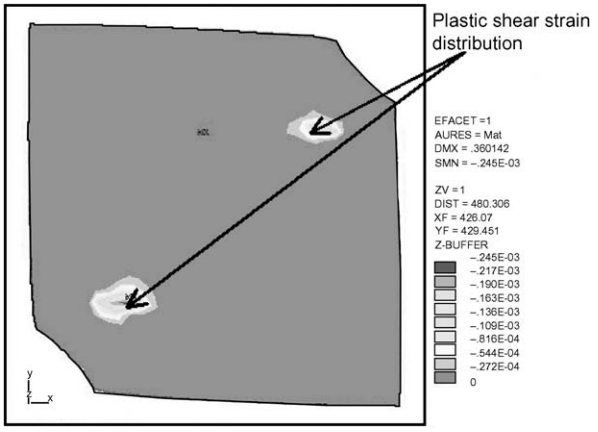

Fig. 13. Plastic shear strain distribution for the simplified isotropic model.

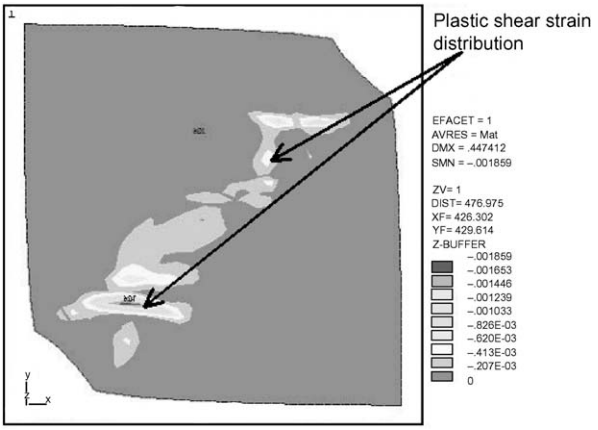

Fig. 14. Plastic shear strain distribution for the simplified orthotropic model.

4.3. Finite element modelling using homogenized medium

The goal of the homogenization is to obtain the mechanical parameters of an equivalent material, based on the establishment of average stresses and strains [18] on a representative volume element (RVE): this is the pattern which is repeated periodically inside the structure (Fig. 15). The average stress σ^0_{ij} and the average strain ε^0_{ij} are defined as:

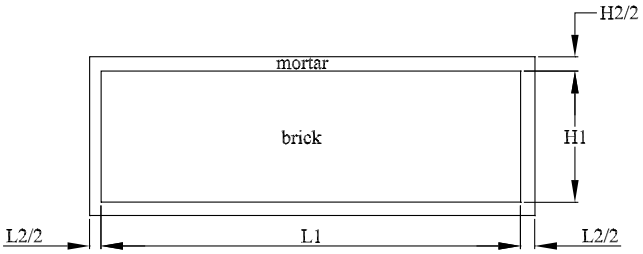

Fig. 15. Representative volume element for the masonry.

$$\sigma_{ij}^0 = \frac{1}{Y}\int_Y \sigma_{ij}\,\mathrm{d}Y = \langle \sigma_{ij}\rangle_Y$$
$$\varepsilon_{ij}^0 = \frac{1}{Y}\int_Y \varepsilon_{ij}\,\mathrm{d}Y = \langle \varepsilon_{ij}\rangle_Y, \tag{2}$$

where Y stands for the RVE. Considering the constitutive law at the RVE level

$$\sigma_{ij} = a_{ijkh}\varepsilon_{kh},$$

the average stress can be expressed as:

$$\sigma_{ij}^0 = \langle a_{ijkh}\varepsilon_{kh}\rangle_Y. \tag{3}$$

On the hypothesis of the existence of a rigorous relation between the strain at the RVE level and the average strain,

$$\varepsilon_{ij} = c_{ijkh}\varepsilon_{kh}^0, \tag{4}$$

it is possible to obtain an averaged constitutive law:

$$\sigma_{ij}^0 = a_{ijkh}^0\varepsilon_{kh}^0, \tag{5}$$

with

$$a_{ijkh}^0 = \langle a_{ijpq}c_{pqkh}\rangle_Y. \tag{6}$$

The goal is to evaluate c_{ijkl}.

In fact, the problem is to find a stress field σ and a displacement field u for a given macroscopic strain field ε^0, knowing that σ and u must verify some periodicity conditions [18]:

- for the stresses:

  $\sigma_{ij} \in SP(Y)$,

  where

  $SP(Y) = \{\sigma_{ij}|$ the vectors $\sigma_{ij}n_j$ are opposite on the opposite edges of $Y\}$

- for the displacements

  $u_i \in DP(Y)$,

  where

  $$DP(Y) = \{u_i|\varepsilon_{ij}(u_i) \text{ periodic}\} = \{u_i|u_i = \varepsilon_{ij}^0 y_j + v_i,\ v_i \text{ periodic}\}.$$

Thus, the displacement field u_i and the stress field σ must be the solution of the following problem:

$$\begin{cases} \sigma_{ij} = a_{ijmn}\varepsilon_{mn} & \text{on } Y \\ \frac{\partial \sigma_{ij}}{\partial y_j} = 0 & \text{on } Y \\ \sigma \in SP(Y), \quad u_i \in DP(Y) & \\ \langle \varepsilon_{ij}(u_i)\rangle = \varepsilon_{ij}^0. & \end{cases} \tag{7}$$

This is a linear problem and therefore the displacement field may be written:

$$u = \hat{v}^{(kh)}\varepsilon^{0(kh)}, \quad k,h = (1,1) \text{ or } (1,2) \text{ or } (2,2), \tag{8}$$

where $\hat{v}^{(kh)}$ is a solution of the problem (7) for the elementary strain field $\varepsilon^{0(kh)}$:

$$\varepsilon^{0(11)} = \begin{bmatrix} 1 & 0 \\ 0 & 0 \end{bmatrix}, \quad \varepsilon^{0(12)} = \begin{bmatrix} 0 & 1/2 \\ 1/2 & 0 \end{bmatrix}, \quad \varepsilon^{0(22)} = \begin{bmatrix} 0 & 0 \\ 0 & 1 \end{bmatrix}. \tag{9}$$

Eq. (9) leads to the tensor c. Indeed

$$\varepsilon(u) = \varepsilon(\hat{v}^{(kh)})\varepsilon^0 \tag{10}$$

and by identification with Eq. (4)

$$c_{ijkh} = \varepsilon_{ij}(\hat{v}^{(kh)}). \tag{11}$$

Therefore, a possible way to resolve this problem is to load the RVE with an elementary and unity average strain field $\varepsilon^{0(kh)}$ and to search the displacement field $\hat{v}^{(kh)}$ that satisfies the periodicity conditions. The displacement field can be written as:

$$\hat{v}_i^{(kh)} = \varepsilon_{ij}^{0(kh)}\breve{y}_j + v_i^{(kh)}, \tag{12}$$

where $v^{(kh)}$ is periodic. Consequently, the knowledge of the displacements $v^{(kh)}$ allows the evaluation of the $\hat{v}^{(kh)}$, necessary for the computing of the averaged elastic constants a_{ijkl}^0. The $v^{(kh)}$ displacement field can be obtained using the following variational approach:

$$\begin{cases} v^{(kh)} & \text{periodic} \\ \int_Y \mathrm{d}y & a_{ijmn}\varepsilon_{mn}(v^{(kh)})\varepsilon_{ij}(\phi) = \int_Y \mathrm{d}y\ a_{ijkh,i}\phi_j \\ & \forall\phi \text{ periodic on } Y. \end{cases} \tag{13}$$

The right-hand side can be identified as the loading of the RVE Y. Given the fact that the elasticity coefficients a_{ijkl} are constant for each material constituting the RVE, this loading becomes a surface loading at the brick-mortar interface. Indeed, the derivation of the elastic constants is equivalent to a derivation in the sense of distributions: the borders of material discontinuities must be loaded with the corresponding "jumps" of the mechanical characteristics. The strain field $\varepsilon_{mn}(v^{(kh)})$ obtained in this manner can be introduced in the relations (13) and (6) that leads, after some calculations, to the following result:

$$a_{ijkh}^0 = \langle a_{ijkh}\rangle_Y + \langle a_{ijmn}\varepsilon_{mn}(v^{(kh)})\rangle_Y. \tag{14}$$

Thus, the homogenized elastic constants are calculated as the sum of two entities: the average on the RVE of the elastic constants of the constituents and the average of the same elastic constants weighted by the strain field arising from the loading of the brick/mortar interface. Accordingly, this is an improvement to the simplified model described in the previous section.

For the calculation of the homogenized elastic constants, we used the finite element software ANSYS with which we evaluated the strain field in the RVE arising from the elementary loads (Fig. 16). A two dimensional

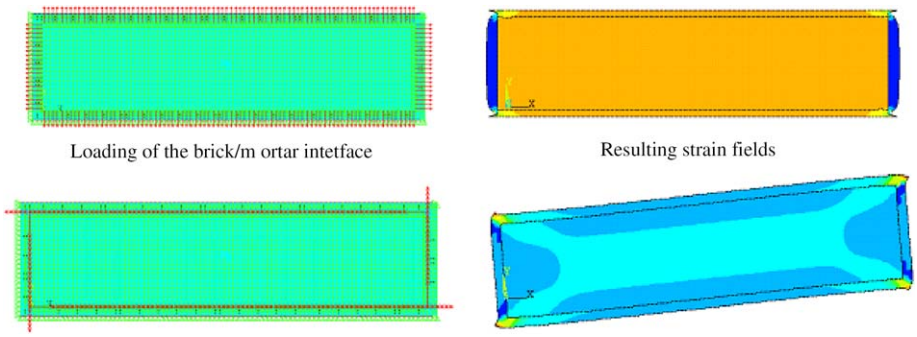

Fig. 16. Finite element modelling of the RVE, loaded with the elastic constant "jumps".

modelling is performed, using four nodes, two degrees of freedom per node and linear interpolation elements. First, an RVE (Fig. 15) is chosen, then the interfaces are loaded with the corresponding elastic constant jumps. Some symmetry conditions are imposed on the border of the RVE for the displacements.

Thus, an elastic orthotropic material is obtained having the elastic moduli: $E_{xx} = 12{,}714$ MPa, in the horizontal direction, and resp. $E_{yy} = 11{,}543$ MPa in the vertical direction. These values correspond to the geometrical configuration of the RVE, since the ratio of brick/mortar is greater in the horizontal direction than that in the vertical one. The values of the elastic moduli for the different models are summarized in Table 4.

Using these values and attributing the Drucker–Prager plasticity parameters of the mortar to the equivalent material we simulated with ANSYS the behaviour of the unreinforced masonry panel for the diagonal compression test.

The force–strain curve for the compressed diagonal (labeled as "homogenized") is presented in the Fig. 12. This curve, compared to the "isotropic" and "orthotropic" curves, is rather close to that of the detailed model (labeled "detailed") where the bricks and the mortar joint are involved. The detailed model, as presented above, shows good correlation with the experimental curve. This finite element simulation confirms the necessity of a homogenization theory and the accuracy of the applied homogenization method. Moreover, the computing time is largely reduced since the mesh size in the case of the homogenized material has at least the size of the RVE.

Table 4
Values of the elastic moduli employed in the finite element modelling

Model	Elastic modulus (MPa)		
	Brick	Mortar	Masonry
Detailed	12,800	4000	–
Isotropic	–	–	9400
Orthotropic	–	–	$E_{xx} = 11{,}600$ $E_{yy} = 9400$
Homogenized	–	–	$E_{xx} = 12{,}714$ $E_{yy} = 11{,}543$

5. Finite element modelling of the reinforced masonry

For the simulation of the behaviour of the reinforced masonry panels we use only the detailed modelling, considering separately the bricks, the mortar and the composite reinforcement. Even if the homogenized model for the unreinforced masonry gives a quite accurate response of the structure, it needs some improvements for taking into account the composite reinforcement. Indeed, for a finite element model of the homogenized medium, the size of the mesh is equal to the size of the RVE. In this condition, the "bonding" of the composite layers on the homogenized medium can't be carried out: as described below, the bonding is realized by coupling the nodes of the composite layer to the nodes of the masonry (or the homogenized medium). Therefore, given the large size of the mesh and the characteristics of the composite layer, an accurate coupling of the nodes is not possible.

5.1. Modelling of the global behaviour

In order to simulate the behaviour of the composite strengthened walls, we considered the detailed modelling of the masonry and a model with elements admitting membrane stiffness and tension-only option for the modelling of the composite layers. This latter is a standard tri-dimensional element having three degrees of freedom at each node. The behaviour law of the composite sheets is considered as elastic: the elastic moduli are determined experimentally (Table 2). The real thicknesses of the composite reinforcements were considered (approximately 2 mm). The model of the reinforced masonry panel is obtained by coupling the nodes of the elements of the masonry with those of composite strips. This corresponds to a perfect bonding between the masonry constituents and the composite strips.

This model allows to describe correctly the overall behaviour of the reinforced panels, for the three studied walls (Figs. 17–19). The evaluation of the elastic domain is not easy for the RFV and RFC reinforced walls because the curves obtained from the simulations are rather parabolic; the experimental ones are rather linear. However, the slope of the curves is in good correlation. For the RFW reinforced wall the two curves coincide.

In these circumstances, it is an interesting issue to study the impact of the geometrical configuration of the composite overlays on the global behaviour of the walls: the goal is to find a configuration which gives an increased deformation capacity. Therefore, we simulated the influence of the geometrical parameters of the composite overlays on the global behaviour of the masonry panels. We present below the results for the RFV type composite obtained for different thicknesses and strip widths.

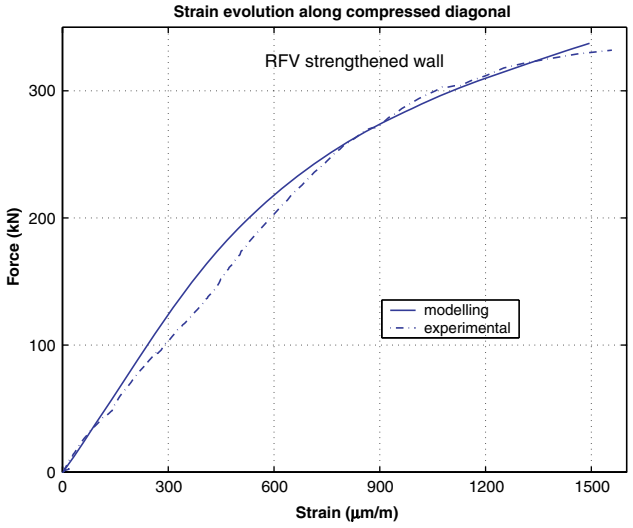

Fig. 17. Numerical and experimental force–strain diagrams for the RFV reinforced wall.

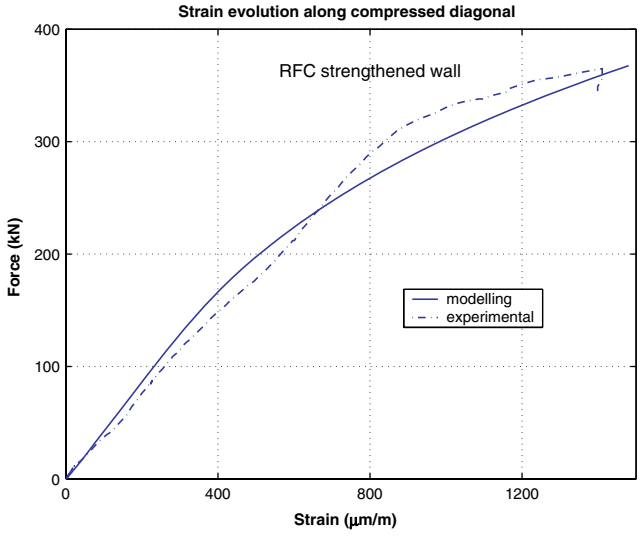

Fig. 18. Numerical and experimental force–strain diagrams for the RFC reinforced wall.

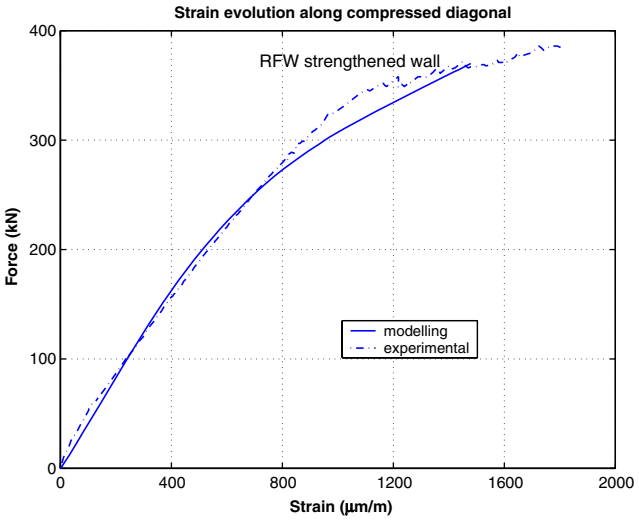

Fig. 19. Numerical and experimental force–strain diagrams for the RFW reinforced wall.

5.2. *Influence of the composite strips configuration on the global behaviour of masonry panels*

We considered three different thicknesses: 1 mm, 2 mm, and respectively 5 mm. We recall that the real thickness of the composite reinforcements is approximately 2 mm, as measured at the time of the tensile tests on coupons. The other dimensions (400×150 mm) and the number of strips were kept unchanged. The force–strain diagrams given by the model show that thicker

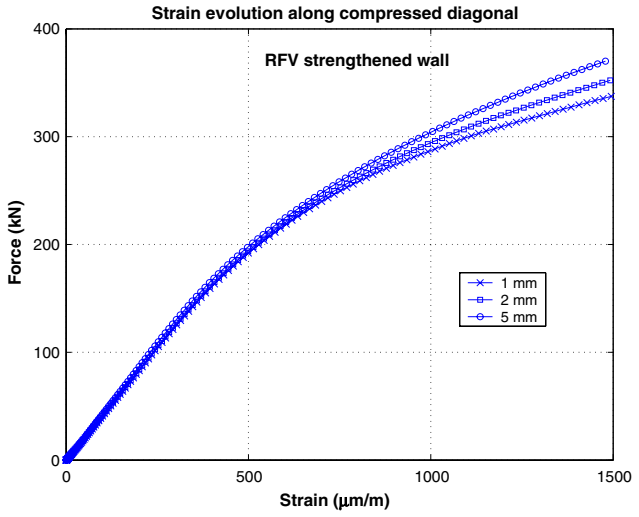

Fig. 20. Numerical force–strain diagrams of the strengthened panels for different thicknesses of the RFV composite.

the composite strip is more the strength of the wall becomes important: the wall which is strengthened with the strips having 5 mm thickness presents a failure load increased with 25% (Fig. 20). On the other hand, the deformation capability is not enhanced by a thicker reinforcement. Besides, we notice also that the reinforcement has no effect on the initial global stiffness of the masonry wall: the slopes of the force–strain curve are identical in spite of composite strips stiffness multiplied by 2 or 5. Therefore, it is not an economical solution to use composites constituted from multiple layers. Indeed, a five times increase of the quantity of the composite produces only a 25% gain on the ultimate force. Moreover, the gain in deformation capability is insignificant: this latter property is essential for seismic design.

These facts emphasize again the utility of the reinforcement applied on the entire surface employing bi-directional composites having low strength and high deformation capabilities (e.g. the RFW type composite). In spite of their mechanical weakness they provide the same strength and a better deformation capability than the other high-strength unidirectional composites.

6. Conclusions

The object of this paper was the finite element modelling of the behaviour of unreinforced and composite material strengthened masonry panels under predominant shear loading. For this purpose we used a commercial software (ANSYS). The accomplishment of the modelling in the prevision of the behaviour of unreinforced walls depends on the appropriate choice of the implemented mechanical parameters. The principal parameters of the chosen formulation have been the elasto-plastic properties of the mortar joint: cohesion and residual friction. The obtained numerical results have been validated experimentally in the case of diagonal compression test of masonry panels. Comparing these results, we remark that finite element modelling gives a realistic image of the behaviour of masonry panels: the ultimate loads, the plastic strain evolution and the failure modes are reproduced with a good approximation. Therefore, the finite element modelling can be a useful tool in the choice of a judicious reinforcement configuration, when technical recommendations are non-existent or in development.

The parametrical study based on the finite element modelling underlined again the effectiveness of bi-directional composites applied on the entire surface, since the increase of the thickness of composite strips that are applied in strips does not induce a proportional increase of the strength or of the deformation capability.

In order to overcome the disadvantages of a detailed modelling in the case of the unreinforced masonry panel, we performed a homogenization of the brick/mortar assemblage. The good correlation between experimental and numerical curves encourages us to use this homogenization method in further works for the study of composite material reinforced masonry structures. In order to improve the finite element modelling, a homogenization of the brick/mortar/composite assemblage is necessary especially when the ''bonding'' of the composite on the homogenized brick/mortar medium can't be realized with a sufficient accuracy. This problem is the subject of further research works.

References

[1] Priestley M, Seible F. Design of seismic retrofit measures for concrete and masonry structures. Construct Build Mater 1995; 9(6):365–77.

[2] Hamelin P. Composite infrastructure applications: concept, design, durability control and prediction. J Compos Technol Res.

[3] Triantafillou T. Seismic retrofitting of structures with fibre-reinforced polymers. Prog Struct Eng Mater 2001;3:57–65.

[4] Evaluation of Earthquake Damaged Concrete and Masonry Wall Buildings-basic procedures, Tech. Rep., Federal Emergency Management Agency (FEMA), 1999.

[5] Ehsani M, Saadatmanesh H, Velasquez J. Behavior of retrofitted URM walls under simulated earthquake loading. J Compos Construct 1999;3(3):134–42.

[6] Albert M, Elwi A, Cheng J. Strengthening of unreinforced masonry walls using FRPs. J Compos Construct 2001;5(2):76–84.

[7] Corradi M, Borri A, Vignoli A. Strengthening techniques tested on masonry structures struck by the Umbria-Marche earthquake of 1997–1998. Construct Build Mater 2002(16):229–39.

[8] Valluzzi M, Tinazzi C, Modena C. Shear behaviour of masonry panels strengthened by FRP laminates. Construct Build Mater 2002:409–16.

[9] Lourenço PB. Computational strategies for masonry structures. Ph.D. thesis, Technical University Delft, Delft University Press, The Netherlands, ISBN 90-407-1221-2, February 1996.

[10] Gambarotta L, Lagomarsino S. Damage models for the seismic response of brick masonry shear walls. Part I: The mortar joint model and its applications. Earthquake Eng Struct Dynam 1997; 26:423–39.

[11] Lee J, Pande G, Midleton J, Kralj B. Numerical modelling of brick masonry panels subject to lateral loadings. Comput Struct 1996;61(4):735–45.

[12] Lopez J, Oller S, Onate E, Lubliner J. A homogeneous constitutive model for masonry. Int J Numer Methods Eng 1999;46: 1651–71.

[13] Gabor A. Contribution à la caractérisation et à la modélisation des maçonneries non-renforcées et renforcées par matériaux composites, Thèse de Doctorat, Université Lyon 1, France, décembre 2002.

[14] Gabor A, Ferrier E, Jacquelin E, Hamelin P. Analysis and modelling of the in-plane shear behaviour of hollow brick masonry panels. Construct Build Mater, in press.

[15] RILEM. LUMB1-Compressive strength of small walls and prisms. Tech Rep, RILEM, 1994.

[16] RILEM. LUMB6-Diagonal tensile strength tests of small wall specimens. Tech Rep, RILEM, 1994.

[17] Gabor A, Ferrier E, Jacquelin E, Hamelin P. Analysis of the in-plane shear behaviour of FRP reinforced hollow brick masonry walls. Struct Eng Mech: An Int J 2005;19(3):237–60.

[18] Suquet P. Plasticité et homogénéisation, Thése de doctorat, Université Pierre et Marie Curie, Paris 6, 1982.